Synthetic and Systems Biotechnology 4 (2019) 49–56

Contents lists available at ScienceDirect

Synthetic and Systems Biotechnology

journal homepage: http://www.keaipublishing.com/synbio

Comparative functional genomics of the acarbose producers reveals potential targets for metabolic engineering

Huixin Xie[1], Qinqin Zhao[1], Xin Zhang, Qianjin Kang, Linquan Bai*

State Key Laboratory of Microbial Metabolism, School of Life Sciences & Biotechnology, Shanghai Jiao Tong University, Shanghai 200240, China

ARTICLE INFO

Keywords:
Acarbose
Comparative genomics
Overproduction
Regulation

ABSTRACT

The α-glucosidase inhibitor acarbose is produced in large-scale by strains derived from *Actinoplanes* sp. SE50 and used widely for the treatment of type-2 diabetes. Compared with the wild-type SE50, a high-yield derivative *Actinoplanes* sp. SE50/110 shows 2-fold and 3–7-fold improvement of acarbose yield and *acb* cluster transcription, respectively. The genome of SE50 was fully sequenced and compared with that of SE50/110, and 11 SNVs and 4 InDels, affecting 8 CDSs, were identified in SE50/110. The 8 CDSs were individually inactivated in SE50. Deletions of *ACWT_4325* (encoding alcohol dehydrogenase) resulted in increases of acarbose yield by 25% from 1.87 to 2.34 g/L, acetyl-CoA concentration by 52.7%, and PEP concentration by 22.7%. Meanwhile, deletion of *ACWT_7629* (encoding elongation factor G) caused improvements of acarbose yield by 36% from 1.87 to 2.54 g/L, transcription of *acb* cluster, and ppGpp concentration to 2.2 folds. Combined deletions of *ACWT_4325* and *ACWT_7629* resulted in further improvement of acarbose to 2.83 g/L (i.e. 76% of SE50/110), suggesting that the metabolic perturbation and improved transcription of *acb* cluster caused by these two mutations contribute substantially to the acarbose overproduction. Enforced application of similar strategies was performed to manipulate SE50/110, resulting in a further increase of acarbose titer from 3.73 to 4.21 g/L. Therefore, the comparative genomics approach combined with functional verification not only revealed the acarbose overproduction mechanisms, but also guided further engineering of its high-yield producers.

1. Introduction

Acarbose (acarviosyl-1,4-maltose), an α-glucosidase inhibitor, is commercially used in the treatment of type-2 diabetes mellitus since 1990, which enables patients to better control the blood sugar level [1–3]. As the high incidence of type-2 diabetes mellitus is becoming a major health problem [4], the constant demand of acarbose and other antidiabetic drugs increases rapidly. The acarbose is produced in large-scale fermentation by strains derived from *Actinoplanes* sp. SE50 [1]. Therefore, improving the productivity of acarbose producers becomes very important nowadays.

Traditionally, strains with high productivity of acarbose used for industrial large-scale fermentation were obtained through multiple rounds of random mutagenesis and screening [5]. *Actinoplanes* sp. SE50/110 is a typical optimized industrial strain derived from SE50 [6]. Recently, its genome was sequenced and analyzed [7], leading to a rapid development of multi-omic analysis, such as transcriptome for comparative gene expression between cells grown in different media, proteome for localization of proteins encoded by the acarbose biosynthetic gene cluster (*acb* cluster), and genome-scale metabolic model for discovery of bottlenecks in acarbose production [8–12]. With the development of efficient genetic manipulation systems for acarbose producing strains [13–15], genetic engineering strategies for further improvement of acarbose productivity are in urgent need.

Comparative genome analysis is frequently used to decipher how the classical mutagenesis-and-screening strategy leads to an improved antibiotic production. The comparative genome study of the wild-type erythromycin producing strain *Saccharopolyspora erythraea* NRRL 2338 and a derived overproducer Px revealed that a considerable number of mutations, affecting genes encoding enzymes involved in central carbon and nitrogen metabolisms, biosynthesis of secondary metabolites, and basic transcription and translation machineries, contribute to erythromycin overproduction [16]. Meanwhile, 250 variations, affecting 227 coding sequences (CDSs), were identified in rifamycin B overproducer *Amycolatopsis mediterranei* HP-130 through comparative genome analysis with the reference strains S699 and U32, and the

Peer review under responsibility of KeAi Communications Co., Ltd.
* Corresponding author.
E-mail address: bailq@sjtu.edu.cn (L. Bai).
[1] These two contributed equally to this work.

https://doi.org/10.1016/j.synbio.2019.01.001
Received 28 October 2018; Received in revised form 31 December 2018; Accepted 10 January 2019

mutations of *mutB2* (coding for the large subunit of methylmalonyl-CoA mutase) and *argS2* (coding for arginyl-tRNA synthetase) were proved to be the causes for rifamycin overproduction [17]. Additionally, the deletions of large fragments including competitive gene clusters and several regulatory genes in salinomycin producer *S. albus* BK 3–25 resulted its overproduction [18]. These approaches take advantage of low-cost genome sequencing and lead to the identification of targets for further titer improvement by genetic engineering [19].

Herein, in order to decipher how the mutagenesis-and-screening method leads to an improved acarbose production, the genome of the wild-type strain SE50 was sequenced and compared with that of the high-yield SE50/110, and the genetic variations were identified. Subsequent functional verification revealed the critical variations responsible for the acarbose overproduction, and the underlying mechanisms were accordingly illustrated. The identified overproduction strategy was applied again in the high-yield strain and resulted in a further improved acarbose yield.

2. Materials and methods

2.1. Bacterial strains, plasmids and media

The strains, plasmids and primers used in this study are listed in Table S1, Table S2 and Table S3, respectively.

Actinoplanes sp. and their derivatives were grown on STY agar medium (sucrose 3%, tryptone 0.5%, yeast extract 0.5%, casin hydrolysate 0.1%, $K_2HPO_4{\cdot}3H_2O$ 0.1%, KCl 0.05%, $FeSO_4$ 0.005%, agar 2%, pH 7.2) at 30 °C for conjugation. For the isolation of total DNA, strains were cultivated in 30 mL SM broth (glucose 1.5%, maltose 1%, $K_2HPO_4{\cdot}3H_2O$ 0.1%, glycerol 1%, maltose extract 1%, tryptone 0.5%, yeast extract 0.5%, casin hydrolysate 0.1%, pH 7.2) in 250-mL baffled flask for 36–48 h on rotary shaker (30 °C, 220 rpm). The *E. coli* ET12567(pUZ8002) was used for conjugation. The *E. coli* cells were cultured in Luria-Bertani (LB) broth with corresponding antibiotics at 37 °C.

2.2. Genome sequencing and assembly of Actinoplanes sp. SE50

The genome of SE50 was sequenced by a combination of Illumina HiSeq 2500 sequencer and PacBio RS II System at Shanghai Biotechnology Corporation, generating one scaffold with 9,239,482 base pairs and providing a 100% coverage. No gap was formed and the obscure base Ns were replaced by PCR amplification using specifically designed PCR primers. Putative protein-coding sequences (CDSs) were predicted by Prodigal_v2.6.1 software. CDS annotation was based on the BLASTP program with NR, COG, and KEGG databases. The single nucleotide variations (SNVs) and InDels were identified by Mummer, Mauve, and BLASTP programs. The whole genome of SE50 has been deposited at GenBank under the accession number CP023298.

2.3. Transcriptome sequencing and comparative analysis of SE50 and SE50/110

The RNA for transcriptome sequencing was sampled on the second day of fermentation. The cells were harvested from 1-mL fermentation culture by centrifuged at 4 °C, put in the liquid nitrogen for 0.5–1 h, and then stored at −80 °C. The RNA extraction, transcriptome sequencing and data analysis were performed by Shanghai Sinomics Corporation. The expression level of each gene was calculated as Fragments Per Kilobase of exon per Megabase of library size (FPKM).

2.4. Fermentation and HPLC analysis of acarbose

The mycelia from SM medium were transferred to 40 mL seed medium (1.5% maltose, 1% glucose, 4% soya flour, 1% glycerol, 1% soluble starch, 0.2% $CaCO_3$, pH 7.2) in baffled flask and cultivated for 20–22 h on rotary shaker at 220 rpm and 30 °C. Then, 7.5 mL seed culture was inoculated to 50 mL fermentation medium (5% maltose, 3% glucose, 1% soya flour, 0.3% glutamate, 0.1% $K_2HPO_4{\cdot}3H_2O$, 0.05% $FeCl_3$ and 0.25% $CaCO_3$, pH 7.2) in 250 mL baffled flask and cultivated for 7–8 days. Additionally, 1 g of glucose and 1 g of maltose were added to each flask at 72 h. The supernatant of fermentation broth was obtained by centrifugation at 12,000 rpm for 10 min, diluted for 3 folds, and analyzed by HPLC (Agilent series 1260, Agilent Technologies, USA). Acarbose was separated with Agilent ZORBAX NH_2 column (4.6 × 250 mm, particle size 5 μm) using an elution buffer composed of acetonitrile and phosphate buffer (0.70 g $Na_2HPO_4{\cdot}12H_2O$ and 0.60 g KH_2PO_4 in 1 L ddH_2O) at a ratio of 65:35 (v/v) with a flow rate of 1 mL/min, and detected at 210 nm.

2.5. RNA extraction and quantitative real-time PCR (qRT-PCR) analysis

Mycelia of *Actinoplanes* spp. were collected at 48 h from fermentation broth, and the total RNA was extracted using Redzol according to the manufacturer's instruction (SBS Genetech, China) [20]. The quality of the RNA was checked by NanoDrop 2000 spectrophotometer. For qRT-PCR experiments, total RNA was reversely transcribed into cDNA using RevertAid™ H Minus First Strand cDNA Synthesis Kit (Thermo Fisher, USA). The qRT-PCR experiments were carried out with a 7500 Fast Real-time RCR system (Applied Biosystems, USA) using Maxima™ SYBR Green/ROX qPCR Maxter Mix (Thermo Fisher, USA) according to the manufacturer's procedure. The transcription of target genes was normalized to the housekeeping gene *hrdB* and quantified by the $2^{-\Delta\Delta CT}$ method [21].

2.6. DNA cloning and gene inactivation

Gene disruption was performed using double crossover homologous recombination strategy. In order to delete the gene *ACWT_4325*, two homologous arms, a 1.66-kb *Xba*I-*Eco*RI fragment of the left flanking region and a 1.49-kb *Eco*RI-*Hin*dIII fragment of the right flanking region were respectively amplified by primers ACWT_4325-L-F/ACWT_4325-L-R and ACWT_4325-R-F/ACWT_4325-R-R from the genome of SE50 and both ligated into *Xba*I/*Hin*dIII-digested pJTU1278-derived replicating vector pLQ751 (Table S2) to generate pLQ903. Then, pLQ903 was transferred into strain SE50 by conjugation from *E. coli* ET12567(pUZ8002). Exconjugants with single-crossover homologous recombination were selected for apramycin and trimethoprim resistance on STY plates. In order to promote double crossover homologous recombination in the exconjugants, the mycelia from STY plates were inoculated to SM broth. Then a 36-h culture was transferred (1/10, v/v) to fresh SM broth for another 36–48 h cultivation. The mycelia were diluted for 10 folds and filtered with non-absorbent cotton wool, and the filtrate was diluted for 10^4-10^5 times. Subsequently, the apramycin-sensitive colonies were selected after cultivation for 4–5 days on STY plates without antibiotics. For further verification, the genotypes of the wild-type, pLQ903, and the mutant candidates were verified by PCR amplification with primers ACWT_4325-F/ACWT_4325-R. The mutants (Δ*4325*) gave a 1.07-kb amplified product, whereas the wild-type gave a 1.88-kb amplified product.

In order to delete the gene *ACWT_7629*, a 1.73-kb *Xba*I-*Eco*RI fragment of the left flanking region and a 1.33-kb *Eco*RI-*Hin*dIII fragment of the right flanking region were respectively amplified by primers ACWT_7629-L-F/ACWT_7629-L-R and ACWT_7629-R-L/ACWT_7629-R-R from the genome of SE50 and both ligated into *Xba*I/*Hin*dIII-digested pLQ751 to generate pLQ906. Then, pLQ906 was transferred into strain SE50 by conjugation from *E. coli* ET12567(pUZ8002). Exconjugants were picked, cultured and screened as described above. The genotypes of the wild-type, pLQ908 and the mutant candidates were verified by PCR amplification with primers ACWT_7629-F/ACWT_7629-R. The mutants (Δ*7629*) gave a 0.62-kb amplified product, whereas the wild-type gave a 0.81-kb amplified

product. Similar methods were used to delete other genes.

2.7. Concentration determination of intracellular ppGpp, acetyl-CoA and phosphoenolpyruvate (PEP)

Mycelia of *Actinoplanes* spp. were collected at 48 h from fermentation media, each sample was centrifuged for 3 min at 12,000 rpm to precipitate the cells. Cell pellets were resuspended in 1 mL 0.9% NaCl and washed by centrifugation for three times. The final pellet was resuspended in 200 mL 0.9% NaCl, to which was added 200 mL 20% formic acid to lyse the cells. The extraction was performed on ice with intermittent vortexing for 15 min and then placed on ice for 30 min. The supernatant of extraction was obtained by centrifugation at 12,000 rpm for 3 min, and 10 μL of supernatant was applied drop-wise onto a polyethyleneimine (PEI)-cellulose TLC plate (Sigma-Aldrich). As a marker, 0.1 mmol of GTP was applied onto the same plate. Chromatography was performed in 1.5 M KH_2PO_4 (pH 3.2) until the buffer front reached the top of the membrane. The plate was dried, and the chromatograms were visualized under UV-light [17,22].

The concentrations of intracellular acetyl-CoA and phosphoenolpyruvate were determined by LC-MS/MS using a modified method [23]. Each strain was inoculated into 30 mL of fermentation medium in triplicate. 1 mL of culture was collected and used to quantify the concentrations of total intracellular proteins [24]. The remaining culture was centrifuged, and the mycelia were instantly quenched and extracted with acetonitrile/methanol/0.1% glacial acetate (45:45:10, v/v) to a final volume of 1 mL at 20 °C. The extraction was performed on ice with intermittent vortexing for 15 min, followed by a 3-min centrifugation at 12,000 rpm and 4 °C. The supernatant (10 μL) was injected for HPLC-MS/MS analysis.

Samples (10 μL) were analyzed by LC-QQQ MS (Agilent 1100 series LC/MSD Trap System) using an Agilent Eclipse TC-C18 column (5 μm, 4.6 × 250 mm). The mobile phase was composed of water with 20 mM ammonium acetate (pH 7.4, solvent A) and methanol with 20 mM ammonium acetate (solvent B). Elution was initiated with constant 25% solvent B for 5 min, and then with a linear gradient from 25% to 100% of solvent B in 10 min, followed by 100% solvent B for 5 min and re-equilibration to initial conditions for 5 min, at a flow rate of 0.5 mL/min [25]. Concentrations of Acetyl-CoA and PEP were measured in a multiple reaction monitoring (MRM) mode with the *m/z* of precursor ion > the *m/z* of product ion (acetyl-CoA 810 > 303, PEP 169 > 81). The ion-trap mass spectrometer was operated with an electro-spray ionization source in positive ion mode. The drying gas flow was 10 L/min with a temperature of 325 °C, and the nebulizer pressure was 30 lb/in^2 [23]. Acetyl-CoA and phosphoenolpyruvate purchased from Sigma were used as standards.

3. Results

3.1. Phenotypic differences between wild-type SE50 and high-yield SE50/110

Actinoplanes sp. SE50/110 is an acarbose-overproducing strain obtained by traditional mutagenesis-and-screening strategy from the wild-type strain SE50. To compare the phenotypic differences of these two producers, the acarbose production, biomass and transcription of genes in *acb* cluster were measured. The acarbose titers of SE50 and SE50/110 were 1.87 g/L and 3.73 g/L, respectively (Fig. 1A). The biomass of SE50 and SE50/110 were 14.60 g/L and 17.80 g/L, respectively (Fig. 1B). Also, the transcription of the genes in the *acb* cluster of SE50/110 was found to be 3–7 fold higher than that of SE50 (Fig. 1C). These results suggested that the substantial increase of acarbose titer of SE50/110 might be resulted from the higher transcription of genes in *acb* cluster.

3.2. Comparative genomics identified DNA variations in the genome of SE50/110

Comparative genome analysis of SE50 and SE50/110 was performed to reveal the genetic basis underlying the acarbose overproduction. While the genome of SE50/110 has been sequenced and submitted to the GenBank (Accession no. CP003170) [7], the whole-genome of SE50 was then fully sequenced with Illumina and PacBio sequencing technologies. After filtering the subreads, 204,594 reads containing 716,835,386 bases were obtained. When combined with the pair-end library sequencing, a single circular chromosome was successfully assembled by SPAdes-3.5.0, comprising 9,239, 482 bp with the average GC content of 71.73%. A total of 8252 protein-coding sequences (CDSs, locus tagged as *ACWT*) were identified by Prodigal_v2.6.1 and further annotated by BLASTP-searching with the NR, COG, and KEGG databases. Additionally, 21 potential secondary metabolite clusters were found to be distributed in the genome of SE50 via antiSMASH analysis [26], and the *acb* cluster is located in the middle region of the chromosome (Fig. S1). Then, the completely annotated genome sequence was submitted to the GenBank (Accession no. CP023298).

Genomic comparison between SE50 and SE50/110 exhibited extremely high similarity in gene content and gene order, and no large fragment deletion occurred in the genome of SE50/110. A total of 115 variations and a 0.55 Mb rearrangement in SE50/110 were initially found and further confirmed by PCR amplification and sequencing. The verification results showed that only 15 mutated sites including 11 SNVs and 4 InDels occurred in the genome of SE50/110 (Fig. 2, Table 1). Other 100 nonexistent variations were attributed to the limited accuracy of the 454 pyrosequencing technology, which were also recently corrected by another research group in the database (GenBank Accession no. NC_017803). Among the 15 identified variations, 8 SNVs and 2 InDels located in coding regions, and 2 InDels and 3 SNVs occurred in intergenic regions, affecting 8 CDSs. The nature of every variation and their proposed functions were listed in Table 1.

Although only a few CDSs are affected in the genome of SE50/110, the comparative transcriptome analysis with SE50 showed obvious differences in gene expression. 1228 and 1337 (~31%) genes were significantly up-regulated and down-regulated ($q < 0.05$, fold-change > 2) in SE50/110, respectively (Fig. 3). Meanwhile, it was remarkable that the transcription of essential genes for acarbose biosynthesis was obviously improved, which was consistent with the results of qRT-PCR analysis (Fig. 1C). Additionally, the transcription of most genes involved in glycolytic pathway and TCA cycle was up-regulated, especially *ACPL_1553* (*gapA*), *ACPL_7704* (*glpX*), *ACPL_549* (*citA*) and *ACPL_7655* (*sdhB*), which might be the major cause for the higher biomass. These results suggested that these variations in the genome of SE50/110 result in prominent perturbation of gene expression and contribute to the cell growth and acarbose production.

Therefore, the roles of 8 affected genes, encoding LacI family transcription regulator (*ACWT_6270*), elongation factor G1 (*ACWT_7629*), alcohol dehydrogenase (*ACWT_4325*), bilirubin oxidase (*ACWT_7246*), ABC transporter (*ACWT_2644*), extracellular matrix-binding protein (*ACWT_4230*), and hypothetical proteins (*ACWT_222* and *ACWT_5166*), were verified by individual deletion in SE50, and the corresponding mutants were named as Δ*222*, Δ*2644*, Δ*4230*, Δ*4325*, Δ*5166*, Δ*6270*, Δ*7246* and Δ*7629*. As shown in Fig. S2, deletion of *ACWT_4325* and *ACWT_7629* resulted in dramatic improvements of acarbose titer. However, no obvious effect on the acarbose titer was observed from other 6 gene deletion mutants. Therefore, we focused on *ACWT_4325* and *ACWT_7629* to elucidate any possible mechanisms for acarbose titer improvement.

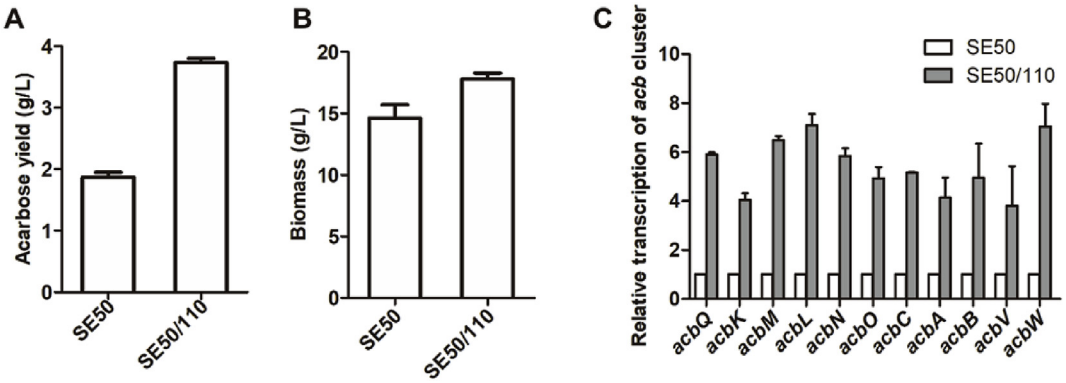

Fig. 1. The phenotypic differences between the wild-type SE50 and the high-yield SE50/110. (A) Acarbose titer of SE50 and SE50/110. (B) Dry cell weight of SE50 and SE50/110. (C) Transcription of genes in *acb* cluster of SE50 and SE50/110 at 48 h during the fermentation process. The Y-axis scale represents the expression of genes. The average transcription of genes in SE50 was set to 1, the transcription of genes in SE50/110 was accordingly calculated. Graphs depict means ± SD. Values represent average results from three independent experiments.

3.3. The metabolic perturbation caused by ACWT_4325 deletion resulted in increases of acarbose titer and intracellular acetyl-CoA and PEP concentrations

ACWT_4325 was predicted as alcohol dehydrogenase that catalyzes the interconversion between ethanol and acetaldehyde. Deletion of *ACWT_4325* resulted in a 25% increase of acarbose titer from 1.87 g/L to 2.34 g/L and 15.5% improvement of the biomass from 14.6 g/L to 16.9 g/L (Fig. 4A–D). However, the transcription of *acb* cluster didn't show obvious increase in mutant Δ*4325* compared with that of SE50 (Fig. S3A). The acarbose titer and biomass were restored to the wild-type levels by trans-complementation of *ACWT_4325* into the Δ*4325* mutant (Fig. 4C and D). Meanwhile, overexpression of *ACWT_4325* in SE50 resulted in simultaneous decrease of acarbose titer and biomass (Fig. S4). These results indicated that inactivation of *ACWT_4325* is beneficial to both acarbose production and cell growth.

The alcohol accumulation branches from acetyl-CoA, a key intermediate bridging the glycolytic pathway and TCA cycle. Therefore, deletion of *ACWT_*4325 might increase the concentration of acetyl-CoA and direct the metabolic flux to TCA cycle, which in turn leads to a better growth. To address this hypothesis, the intracellular acetyl-CoA concentration was quantified and found to be improved by 52.7% in Δ*4325* when compared with that of SE50, which was comparable to that of SE50/110 (Fig. 4E). To determine whether the increase of acetyl-CoA pool also affects the accumulation of phosphoenolpyruvate (PEP), which is involved in the biosynthesis of the acarbose precursor heptulose-7-phosphate, the concentrations of intracellular PEP were quantified and found to be increased by 22.7% in Δ*4325* when compared with that of SE50 (Fig. 4F). These results suggested that the metabolic perturbation caused by the deletion of *ACWT_4325* promotes both acarbose titer and biomass.

3.4. The stringent response caused by ACWT_7629 deletion resulted in acarbose titer and acb gene transcription improvements

Although the production of acarbose was greatly increased by the deletion of *ACWT_4325*, the mutant didn't show obvious improvement in the transcription of genes in *acb* cluster, implying that the distinct difference on the transcription of *acb* cluster between SE50 and SE50/110 is caused by other mutations. Deletion of gene *ACWT_7629*,

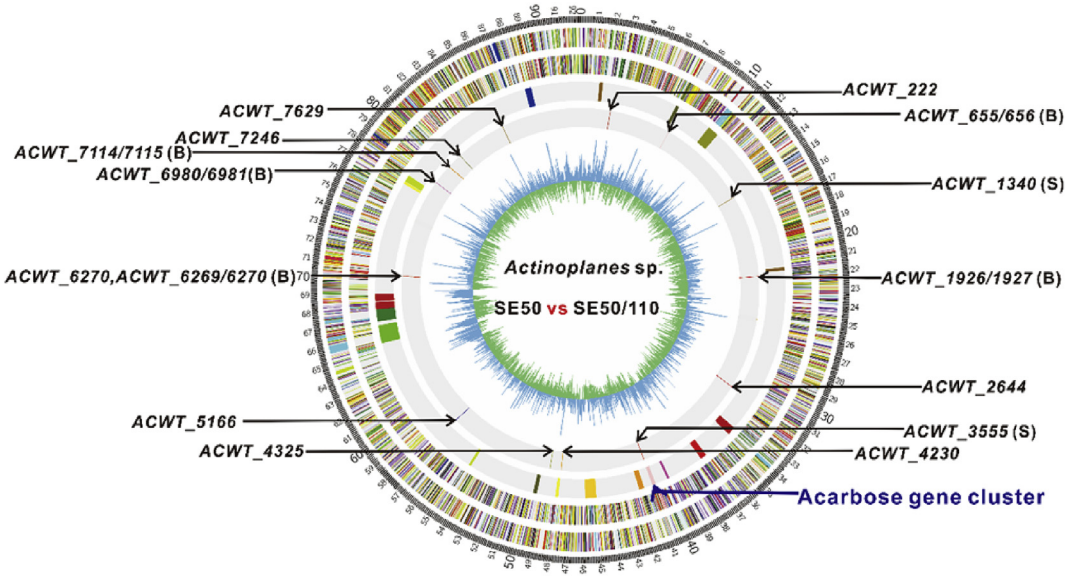

Fig. 2. Chromosome map of genetic variations distinguishing *Actinoplanes* sp. SE50/110 from SE50. From the outside in, Circle 1 and 2: (forward and reverse strands), predicted protein coding sequences colored according to COG function categories; Circle 3: distribution of secondary metabolic gene clusters; Circle 4: positions of variations between SE50/110 and SE50; Circle 5: GC content. Position of acarbose biosynthetic gene cluster was marked with arrow. S: synonymous variations. B: variations in intergenic regions.

Table 1
The SNVs and InDels in the genome of high-yield SE50/110 compared with the wild-type SE50.

Gene_ID in SE50	Variation type	Gene_ID in SE50/110	Protein functions
ACWT_222	snv	*ACPL_337*	hypothetical protein
ACWT_2644	snv	*ACPL_2902*	ABC transporter
ACWT_4230	del	*ACPL_4359*	extracellular matrix-binding protein
ACWT_4325	snv	*ACPL_4454*	alcohol dehydrogenase
ACWT_5166	del	*ACPL_5296*	hypothetical protein
ACWT_6270	snv	*ACPL_6403*	LacI family transcription regulator
ACWT_7246	snv	*ACPL_7376*	bilirubin oxidase
ACWT_7629	snv	*ACPL_7760*	elongation factor G1
ACWT_1340	snv (S)	*ACPL_1461*	amine oxidase
ACWT_3555	snv (S)	*ACPL_3683*	α-amlyase
ACWT_655/ACWT_656	snv (B)	*ACPL_772/ACPL_773*	large subunit ribosomal protein L7/L12 DNA-directed RNA polymerase β subunit
ACWT_1926/ACWT_1927	snv (B)	*ACPL_2048/ACPL_2049*	transcriptional attenuator/selenoprotein W-related protein
ACWT_6269/ACWT_6270	del (B)	*ACPL_6402/ACPL_6403*	maltotriose-binding protein/LacI family transcription regulator
ACWT_6980/ACWT_6981	snv (B)	*ACPL_7111/ACPL_7112*	hypothetical protein/hypothetical protein
ACWT_7114/ACWT_7115	del (B)	*ACPL_7244/ACPL_7245*	ArsR family transcriptional regulator/PadR family transcriptional regulator

snv, single nucleotide variation; del, deletion; S, synonymous variation; B, variation in intergenic region.

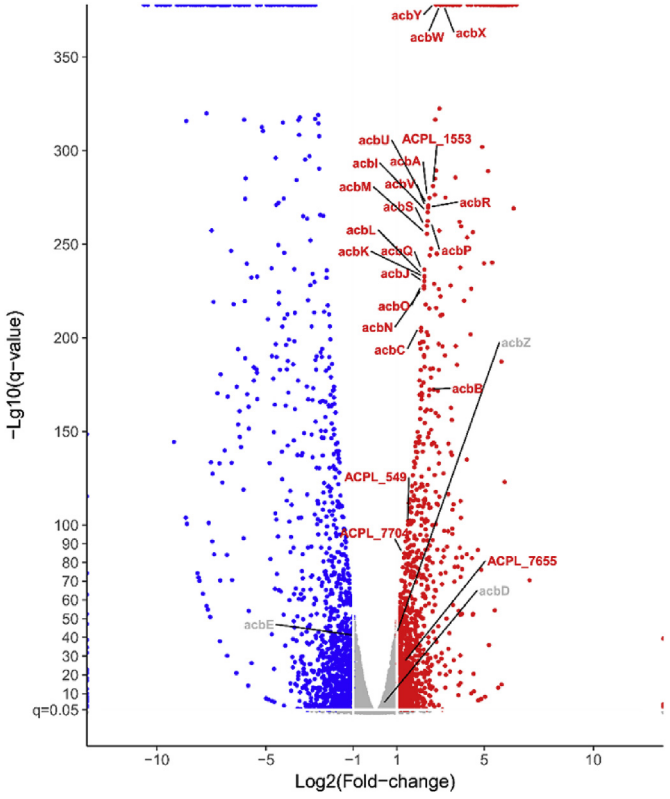

Fig. 3. Comparative transcriptome analysis of SE50 and SE50/110. The volcano plot shows the differential gene expression in SE50/110 when compared with that in SE50. The data point above the significance threshold ($q < 0.05$, fold-change > 2) are marked in blue (down-regulated in SE50/110) and red (up-regulated in SE50/110), and others are marked in gray (not significant). Genes mentioned in the text are shown near their corresponding spots. (For interpretation of the references to color in this figure legend, the reader is referred to the Web version of this article.)

predicated as elongation factor G protein, was crucial for acarbose overproduction, showing 36% improvement of acarbose titer from 1.87 g/L to 2.54 g/L (Fig. 5A–C). Meanwhile, the transcription of the genes in *acb* cluster was showed 2–5-fold increase in Δ*7629* compared with that of SE50, which were comparable to that of SE50/110 (Fig. 5D). However, the biomass of Δ*7629* was slightly less than that of SE50 (Fig. S5). Subsequently, the acarbose titer, transcription of *acb* cluster and cell growth were all restored to the wild-type levels by trans-complementation of *ACWT_7629* into Δ*7629* mutant (Fig. 5C–D, Fig. S5). These results indicated that the transcription increase of *acb* cluster caused by *ACWT_7629* deletion leads to the acarbose overproduction.

Elongation factors are essential proteins involved in translation process in bacteria [27]. Inactivation of the elongation factors in *Salmonella typhimurium* has been proved to cause slow growth and accumulation of large amount of ppGpp (guanosine 3′, 5′ bipyrophosphate), a signaling molecule of bacterial stringent response [22]. The less biomass and obviously up-regulated *acb* cluster transcription of Δ*7629* led us to hypothesize that the deletion of *ACWT_7629* causes an increase of intracellular ppGpp concentration, which in turn promotes the transcription of *acb* cluster as well as the acarbose production. To verify this hypothesis, intracellular ppGpp concentrations were quantified and found to be 2.2-fold improved in Δ*7629* compared with that of SE50, which was comparable to that of SE50/110 (Fig. 5E).

3.5. Combined deletions of ACWT_4325 and ACWT_7629 further improved acarbose production

Since the acarbose titer was substantially improved in both Δ*4325* and Δ*7629* mutants, deletion of gene *ACWT_4325* was further performed in the mutant Δ*7629*. The mutant was named as Δ*4325*/Δ*7629*, which showed further enhancement of acarbose titer, reaching 2.83 g/L (i.e. 76% of SE50/110) (Fig. 6A). Also, the biomass of Δ*4325*/Δ*7629* was relatively higher than that of SE50, although it is less than that of Δ*4325* (Fig. 6B). Additionally, the transcription of *acb* gene was substantially increased in the Δ*4325*/Δ*7629* mutant when compared with that of SE50 (Fig. 6C), which was comparable to that of Δ*7629* and SE50/110. Therefore, the metabolic perturbation and improved *acb* gene transcription caused by *ACWT_4325* and *ACWT_7629* mutations remarkably contributed to acarbose overproduction in SE50/110.

3.6. Enforced application of similar strategies for further acarbose titer increase in SE50/110

To further improve acarbose titer in SE50/110, similar overproduction strategies were utilized by inactivation of genes homologous to *ACWT_4325* and *ACWT_7629*. According to the protein function annotation and gene transcriptions, *ACPL_2718*, *ACPL_3172*, *ACPL_5664* and *ACPL_6548* were chosen to be individually inactivated in SE50/110 to generate the corresponding mutants named as Δ*2718*, Δ*3172*, Δ*5664* and Δ*6548*. Inactivation of *ACPL_3172*, showing certain similarity with *ACWT_4325*, resulted in a 12.9% improvement of acarbose titer from 3.73 g/L to 4.21 g/L (Fig. 7A). Besides, the biomass of Δ*3172* mutant was higher than that of SE50/110 (Fig. 7B).

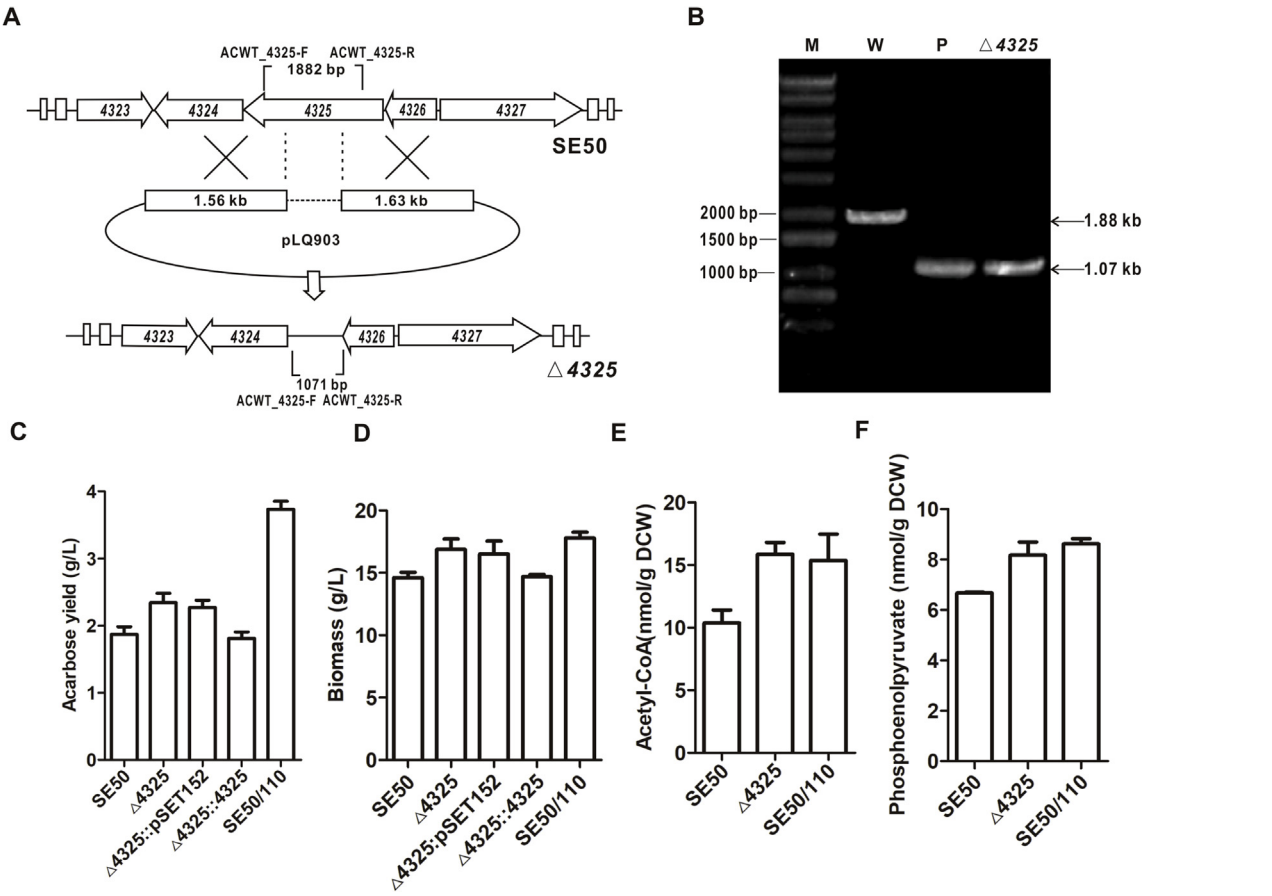

Fig. 4. The effect of deletion of *ACWT_4325* on acarbose titer, biomass and intracellular metabolites. (A) Schematic representation of homologous recombination of *ACWT_4325* deletion. (B) Confirmation of the mutant Δ4325 by PCR amplification. The mutant Δ*4325* gave a 1.07-kb product, whereas the wild-type SE50 gave a 1.88-kb product. (C) Acarbose titers of SE50, Δ*4325,* Δ*4325*:pSET152, Δ*4325*:*4325* and SE50/110. (D) Biomass of SE50, SE50/110 and the mutants. (E) The concentrations of intracellular acetyl-CoA in SE50, Δ*4325* and SE50/110. (F) The concentrations of intracellular phosphoenolpyruvate in SE50, Δ*4325* and SE50/110. Graphs depict means ± SD. Values represent average results from three independent experiments.

4. Discussion

In order to understand the mechanism underlying the higher acarbose productivity in SE50/110, the whole genome of SE50 was sequenced (Fig. S1) and compared with the genome of SE50/110, which was published in 2012 [7]. Even though 115 mutated sites were initially identified in the genome of SE50/110, only 15 mutated sites were confirmed to be existed in SE50/110 via intensive PCR amplification and sequencing verification (Fig. 2, Table 1). During the manuscript preparation, these errors were recently corrected, and the genome sequence of SE50/110 was refined by whole-genome re-sequencing [28], which confirmed the high accuracy of our sequencing data.

In this work, deletion of carbohydrate metabolism related gene *ACWT_4325* led to the improvement of acarbose titer, biomass, and intracellular concentrations of acetyl-CoA and PEP (Fig. 4C–F). This finding suggested that metabolic perturbation caused by *ACWT_4325* deletion played a vital role in acarbose production. To further correlate the metabolite concentrations and the acarbose production, concentration of 2-*epi*-5-*epi*-valiolone in the fermentation broth, as the first intermediate in acarbose biosynthesis, was determined. Although no obvious change was found at 48 h of fermentation, the concentration of 2-*epi*-5-*epi*-valiolone of Δ*4325* was improved for 3 folds after 7-day fermentation, suggesting that deletion of *ACWT_4325* increased the flux from acetyl-CoA via PEP to the ultimate acarbose biosynthesis (Fig. S3B).

The guanosine tetraphosphate (ppGpp) [30,31], as the signaling molecule of stringent response, has been proved to play a central role in triggering the onset of secondary metabolism in actinomycetes [32]. For example, the production of glycopeptide antibiotic A40926 in *Actinomadura* sp. ATCC 39727 was dependent on the control of gene transcription by the stringent response [33]. In addition, specific mutations in the *rpoB* gene (encoding the RNA polymerase β-subunit) of *S. lividans* exerted function at the transcription level by activating directly or indirectly key regulatory genes, including *actII-ORF4* and *red*, to achieve the productions of actinorhodin and/or prodigiosins, which was proposed to mimic the ppGpp-bound form in activating the secondary metabolism [34]. Meanwhile, the mutation of translation elongation factor Tu (EF-Tu) has been proved to affect the cell growth and increase the ppGpp concentration in *Salmonella typhimurium* [22]. In our work, deletion of EF-G in *Actinoplanes* spp. was confirmed to increase intracellular ppGpp and then lead to the enhancement of *acb* gene transcription.

In summary, our work disclosed the genetic mechanisms underlying the acarbose overproduction in SE50/110 through comparative genomics and functional verification. The metabolic perturbation and stringent response caused by mutations resulted in substantial increases of cell growth, supply of precursor, and transcription of genes in *acb* cluster. Additionally, enforced application of one of these two strategies resulted in a further increased acarbose titer in SE50/110. The comparative genome approach and mechanisms underlying acarbose overproduction reported in this work would shed lights on the overproduction and genetic engineering of other microbial secondary metabolites.

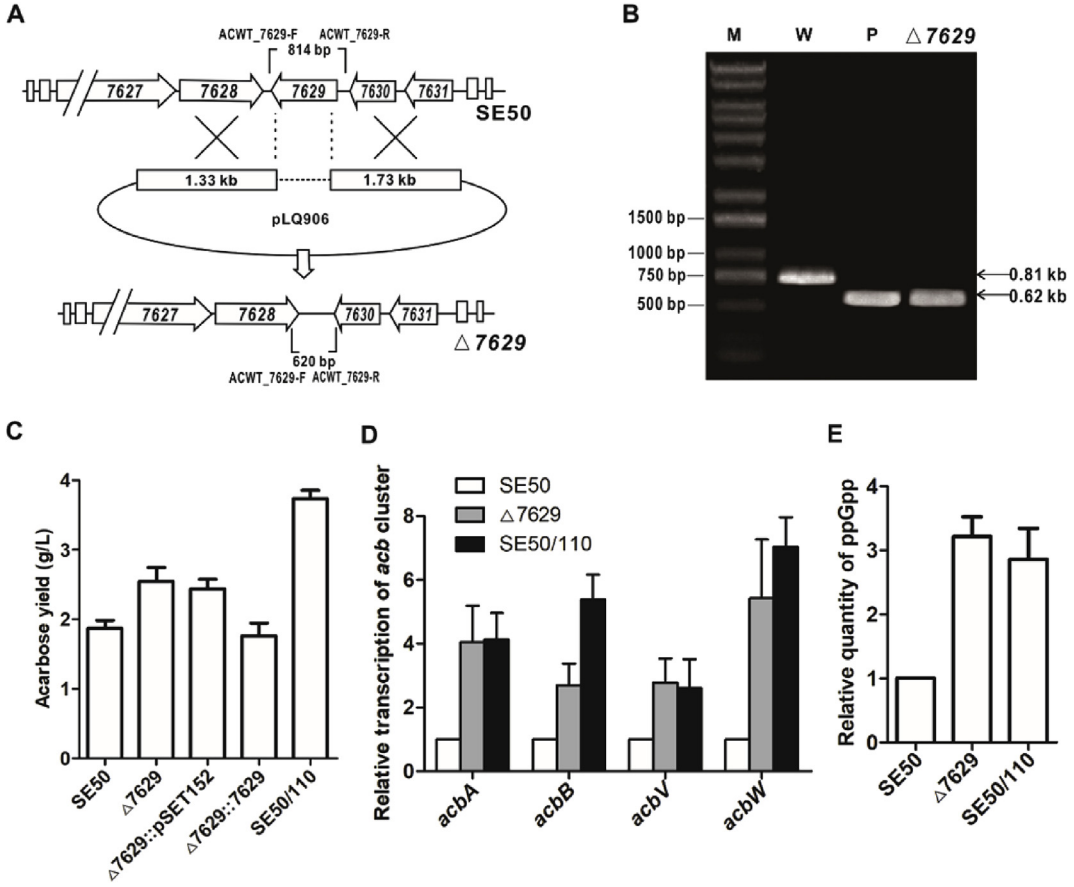

Fig. 5. The effect of deletion of *ACWT_7629* on acarbose titer, *acb* cluster transcription and ppGpp concentration. (A) Schematic representation of homologous recombination of *ACWT_7629* deletion. (B) Confirmation of Δ7629 by PCR amplification. The mutant Δ*7629* gave a 0.62-kb product, whereas the wild-type SE50 gave a 0.81-kb product. (C) Acarbose titers of SE50, Δ*7629*, Δ*7629*:pSET152, Δ*7629*:*7629* and SE50/110. (D) Transcription of genes in *acb* cluster of SE50, Δ*7629* and SE50/110. (E) The relative intracellular concentrations of ppGpp in SE50, Δ*7629* and SE50/110. Graphs depict means ± SD. Values represent average results from three independent experiments.

Accession number

The genome sequence of *Actinoplanes* sp. SE50 has been deposited at GenBank under the accession number CP023298.

Conflicts of interest

The authors declare that they have no competing interests.

Acknowledgements

This work was supported by grants from the National Natural Science Foundation of China (No. 31470157, 21661140002, 31830104, U1703236), and the Shanghai Science and Technology Committee (No. 17JC1403600). We are grateful to Dr. Weishan Wang and the late Professor Keqian Yang (Institute of Microbiology, Chinese Academy of Sciences) for kindly providing the promoter *kasO*p*.

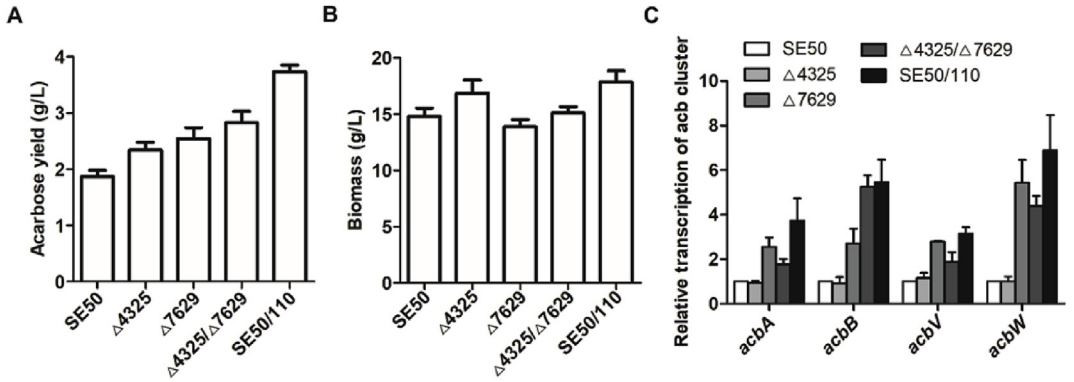

Fig. 6. Effects of combined deletions of *ACWT_4325* and *ACWT_7629* on acarbose titer, biomass and transcription of genes in *acb* cluster. (A) Acarbose titers of SE50, Δ*4325*, Δ*7629*, Δ*4325*/Δ*7629* and SE50/110. (B) Biomass of SE50, SE50/110 and these mutants. (C) Transcription of genes in *acb* cluster of SE50, SE50/110 and mutants. Graphs depict means ± SD. Values represent average results from three independent experiments.

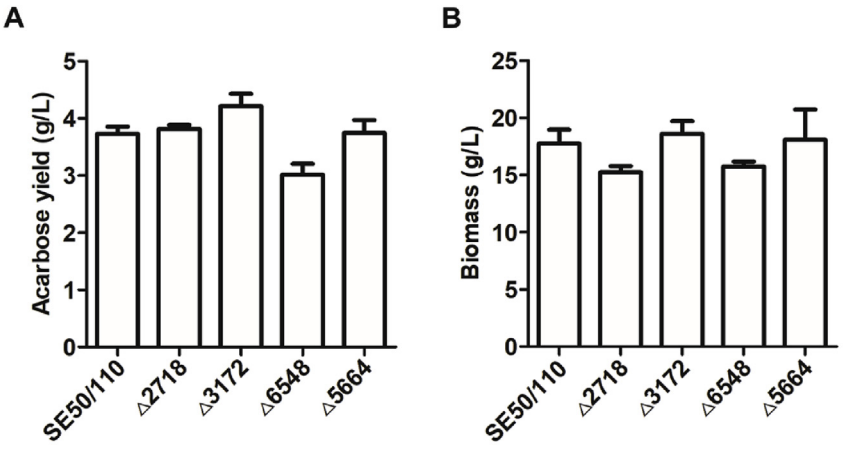

Fig. 7. Effects of Individual deletion of genes in SE50/110 on acarbose titer and biomass. Δ*2718*, deletion of *ACPL_2718*. Δ*3172*, deletion of *ACPL_3172*. Δ*6548*, deletion of *ACPL_6548*. Δ*5664*, deletion of *ACPL_5664*. (A) Acarbose titers of SE50/110 and mutants. (B) Biomass of SE50/110 and mutants. Graphs depict means ± SD. Values represent average results from three independent experiments.

Appendix A. Supplementary data

Supplementary data to this article can be found online at https://doi.org/10.1016/j.synbio.2019.01.001.

References

[1] Wehmeier UF, Piepersberg W. Biotechnology and molecular biology of the α-glucosidase inhibitor acarbose. Appl Microbiol Biotechnol 2004;63:613–25. https://doi.org/10.1007/s00253-003-1477-2.

[2] Bischoff H. Pharmacology of α-glucosidase inhibition. Eur J Clin Investig 1994;24(Suppl 3):3.

[3] Prout TE. Intensive blood glucose control and vascular outcomes in patients with type 2 diabetes. N Engl J Med 2008;358:2560–72. https://doi.org/10.1016/j.ecl.2017.10.002.

[4] Chiasson JL, Josse RG, Gomis R, Hanefeld M, Karasik A, Laakso M, et al. Acarbose for prevention of type 2 diabetes mellitus: the STOP-NIDDM randomised trial. Lancet 2002;359:2072. https://doi.org/10.1016/S0140-6736(02)08905-5.

[5] Feng ZH, Wang YS, Zheng YG. A new microtiter plate-based screening method for microorganisms producing α-amylase inhibitors. Biotechnol Bioproc Eng 2011;16:894–900. https://doi.org/10.1007/s12257-011-0033-7.

[6] Wehmeier UF. The Biosynthesis and metabolism of acarbose in *Actinoplanes* sp. SE 50/110: a progress report. Biocatal Biotransform 2003;21:279–85. https://doi.org/10.1080/10242420310001614388.

[7] Schwientek P, Szczepanowski R, Rückert C, Kalinowski J, Klein A, Selber K, et al. The complete genome sequence of the acarbose producer *Actinoplanes* sp. SE50/110. BMC Genomics 2012;13:112. https://doi.org/10.1186/1471-2164-13-112.

[8] Wendler S, Otto A, Ortseifen V, Bonn F, Neshat A, Schneiker-Bekel S, et al. Comprehensive proteome analysis of *Actinoplanes* sp. SE50/110 highlighting the location of proteins encoded by the acarbose and the pyochelin biosynthesis gene cluster. J Proteom 2015;125:1–16. https://doi.org/10.1016/j.jprot.2015.04.013.

[9] Wendler S, Otto A, Ortseifen V, Bonn F, Neshat A, Schneiker-Bekel S, et al. Comparative proteome analysis of *Actinoplanes* sp. SE50/110 grown with maltose or glucose shows minor differences for acarbose biosynthesis proteins but major differences for saccharide transporters. J Proteom 2016;131:140. https://doi.org/10.1016/j.jprot.2015.10.023.

[10] Wendler S, Hürtgen D, Kalinowski J, Klein A, Niehaus K, Schulte F, et al. The cytosolic and extracellular proteomes of *Actinoplanes* sp. SE50/110 led to the identification of gene products involved in acarbose metabolism. J Biotechnol 2013;167:178.

[11] Schwientek P, Wendler S, Neshat A, Eirich C, Rückert C, Klein A, et al. Comparative RNA-sequencing of the acarbose producer *Actinoplanes* sp. SE50/110 cultivated in different growth media. J Biotechnol 2013;167:166–77. https://doi.org/10.1016/j.jbiotec.2012.10.019.

[12] Wang Y, Xu N, Ye C, Liu L, Shi Z, Wu J. Reconstruction and in silico analysis of an *Actinoplanes* sp. SE50/110 genome-scale metabolic model for acarbose production. Front Microbiol 2015;6:632. https://doi.org/10.3389/fmicb.2015.00632.

[13] Gren T, Ortseifen V, Wibberg D, Schneikerbekel S, Bednarz H, Niehaus K, et al. Genetic engineering in *Actinoplanes* sp. SE50/110 -development of an intergeneric conjugation system for the introduction of actinophage-based integrative vectors. J Biotechnol 2016;232:79–88. https://doi.org/10.1016/j.jbiotec.2016.05.012.

[14] Wolf T, Gren T, Thieme E, Wibberg D, Zemke T, Pühler A, et al. Targeted genome editing in the rare actinomycete *Actinoplanes* sp. SE50/110 by using the CRISPR/Cas9 system. J Biotechnol 2016;231:122–8. https://doi.org/10.1016/j.jbiotec.2016.05.039.

[15] Zhao Q, Xie H, Peng Y, Wang X, Bai L. Improving acarbose production and eliminating the by-product component C with an efficient genetic manipulation system of *Actinoplanes* sp. SE50/110. Synth Syst Biotechnol 2017;2:302–9. https://doi.org/10.1016/j.synbio.2017.11.005.

[16] Peano C, Talà A, Corti G, Pasanisi D, Durante M, Mita G, et al. Comparative genomics and transcriptional profiles of *Saccharopolyspora erythraea* NRRL 2338 and a classically improved erythromycin over-producing strain. Microb Cell Fact 2012;11:32. https://doi.org/10.1186/1475-2859-11-32.

[17] Peano C, Damiano F, Forcato M, Pietrelli A, Palumbo C, Corti G, et al. Comparative genomics revealed key molecular targets to rapidly convert a reference rifamycin-producing bacterial strain into an overproducer by genetic engineering. Metab Eng 2014;26:1–16. https://doi.org/10.1016/j.ymben.2014.08.001.

[18] Zhang X, Lu C, Bai L. Mechanism of salinomycin overproduction in *Streptomyces albus* as revealed by comparative functional genomics. Appl Microbiol Biotechnol 2017;101:4635–44. https://doi.org/10.1007/s00253-017-8278-5.

[19] Rothberg JM, Leamon JH. The development and impact of 454 sequencing. Nat Biotechnol 2008;26:1117. https://doi.org/10.1038/nbt1485.

[20] Lu C, Wu H, Su X, Bai L. Elimination of indigenous linear plasmids in *Streptomyces hygroscopicus* var. *jinggangensis* and *Streptomyces* sp. FR008 to increase validamycin A and candicidin productivities. Appl Microbiol Biotechnol 2017;101:4247–57. https://doi.org/10.1007/s00253-017-8165-0.

[21] Livak KJ, Schmittgen TD. Analysis of relative gene expression data using real-time quantitative PCR and the $2^{-\Delta\Delta CT}$ method. Methods 2001;25:402–8. https://doi.org/10.1006/meth.2001.1262.

[22] Bergman JM, Hammarlöf DL, Hughes D. Reducing ppGpp level rescues an extreme growth defect caused by mutant EF-Tu. PLoS One 2014;9:e90486https://doi.org/10.1371/journal.pone.0090486.t001.

[23] Armando JW, Boghigian BA, Pfeifer BA. LC-MS/MS quantification of short-chain acyl-CoA's in *Escherichia coli* demonstrates versatile propionyl-CoA synthetase substrate specificity. Lett Appl Microbiol 2012;54:140–8. https://doi.org/10.1111/j.1472-765X.2011.03184.x.

[24] Tan GY, Peng Y, Lu C, Bai L, Zhong JJ. Engineering validamycin production by tandem deletion of γ-butyrolactone receptor genes in *Streptomyces hygroscopicus* 5008. Metab Eng 2015;28:74–81. https://doi.org/10.1016/j.ymben.2014.12.003.

[25] Lu C, Zhang X, Jiang M, Bai L. Enhanced salinomycin production by adjusting the supply of polyketide extender units in *Streptomyces albus*. Metab Eng 2016;35:129–37. https://doi.org/10.1016/j.ymben.2016.02.012.

[26] Weber T, Kai B, Duddela S, Krug D, Kim HU, Bruccoleri R, et al. antiSMASH 3.0-a comprehensive resource for the genome mining of biosynthetic gene clusters. Nucleic Acids Res 2015;43:W237–43. https://doi.org/10.1093/nar/gkv437.

[27] Hughes D, Tubulekas I. Ternary complex-ribosome interaction: its influence on protein synthesis and on growth rate. Biochem Soc Trans 1993;21:851.

[28] Wolf T, Schneiker-Bekel S, Neshat A, Ortseifen V, Wibberg D, Zemke T, et al. Genome improvement of the acarbose producer *Actinoplanes* sp. SE50/110 and annotation refinement based on RNA-seq analysis. J Biotechnol 2017;251. https://doi.org/10.1016/j.jbiotec.2017.04.013.

[30] Chakraburtty R, White J, Takano E, Bibb M. Cloning, characterization and disruption of a (p)ppGpp synthetase gene (*relA*) of *Streptomyces coelicolor* A3(2). Mol Microbiol 1996;19:357.

[31] Takano E, Bibb MJ. The Stringent response, ppGpp and antibiotic production in *Streptomyces coelicolor* A3(2). Actinomycetologica 1994;8:1–16.

[32] Ochi K. From microbial differentiation to ribosome engineering. Biosci Biotechnol Biochem 2007;71:1373. https://doi.org/10.1271/bbb.70007.

[33] Vigliotta G, Tredici SM, Damiano F, Montinaro MR, Pulimeno R, Summa RD, et al. Natural merodiploidy involving duplicated *rpoB* alleles affects secondary metabolism in a producer actinomycete. Mol Microbiol 2005;55:396. https://doi.org/10.1111/j.1365-2958.2004.04406.x.

[34] Hu H, Zhang Q, Ochi K. Activation of antibiotic biosynthesis by specified mutations in the *rpoB* gene (encoding the RNA polymerase β subunit) of *Streptomyces lividans*. J Bacteriol 2002;184:3984. https://doi.org/10.1128/JB.184.14.3984-3991.2002.